

The Maxwell spectrum bifurcation on the Schwarzschild black holes in a cavity with vanishing energy flux boundary conditions

Yunhe Lei, Mengjie Wang,^{*} and Jiliang Jing

*Department of Physics and Synergetic Innovation Center for Quantum Effects and Applications,
Hunan Normal University, Changsha, Hunan 410081, P.R. China*

(Dated: May 18, 2022)

We perform a systematic study of the Maxwell quasinormal spectrum in a mirror-like cavity following the generic vanishing energy flux principle, by starting with the Schwarzschild black holes in this paper. The vanishing energy flux principle leads to *two* different sets of boundary conditions and therefore, *two* different sets of modes. In a pure cavity, the Maxwell equations are solved analytically and we obtain two distinct sets of normal modes, which is contradictory to the counterpart of the anti-de Sitter (AdS) case. For the case of black holes in a cavity, we solve the Maxwell equations numerically and the Maxwell spectrum is explored by varying the mirror radius r_m , the angular momentum quantum number ℓ , and the overtone number N . In particular, we proclaim that the Maxwell spectrum may *bifurcate* for both boundary conditions when the mirror is placed around the black hole event horizon, which is analogous to the spectrum bifurcation effects found for the Maxwell fields on asymptotically AdS black holes. This observation provides another example to exhibit the similarity between black holes in a cavity and the AdS black holes.

I. INTRODUCTION

Black holes (BHs) are predicted by General Relativity (GR), and the existence of BHs has been confirmed by the observations of gravitational waves [1–6] and black hole shadow [7–10], as the direct evidences. While quasinormal modes (QNMs) play vital roles in both of the aforementioned observations. For the former case, QNMs determine the ringdown phase of gravitational waves [11, 12]; and for the latter case, in the eikonal limit, the real part of QNMs is related to the radius of the BH shadow and the imaginary part is related to the amplitude ratio between the n th image and the $(n+2)$ th image [13, 14].

Black hole quasinormal modes have been extensively studied, both in GR and in alternative theories of gravity, for different spin fields on various backgrounds, see for example [15–18] and references therein. To obtain QNMs, one has to solve perturbation equations with proper boundary conditions at the asymptotic regions. At the event horizon, ingoing wave boundary conditions are commonly imposed. Boundary conditions at the other asymptotic region, however, are varied with the asymptotic structure of the background spacetimes. For asymptotically flat (de Sitter) spacetimes, QNMs are defined as outgoing wave boundary conditions at infinity (the cosmological horizon). For asymptotically anti-de Sitter (AdS) spacetimes, on the other hand, boundary conditions at infinity are typically imposed with the Dirichlet type boundary conditions, as shown for scalar fields [19–21]. These boundary conditions are also generalized to other spin fields [22–27] but with a few issues. The Dirichlet type scalar-like boundary conditions *cannot*: (i) be applied to the Teukolsky variables even in a

spherically symmetric background; (ii) produce normal modes for the Dirac fields on pure AdS spacetimes. To overcome these issues, recently we have proposed the vanishing energy flux principle to calculate QNMs [28–34]. We unveil, for asymptotically AdS BHs, that the vanishing energy flux principle leads to *two* distinct branches of QNMs for both the Maxwell [28–31] and the Dirac fields [33, 34], and uncover the spectrum bifurcation effects for the Maxwell fields [30].

The vanishing energy flux principle originates from the fact that the asymptotic AdS boundary acts like a perfectly reflecting mirror [28]. From this viewpoint, one may expect that this principle is also applicable to a BH-mirror system. In this paper we will show that this is indeed the case.

We shall initialize a systematic study on the quasinormal spectrum of spin fields around BHs in a mirror-like cavity, under the vanishing energy flux principle. As the first paper in this direction, here we focus on the Maxwell fields interacting with the Schwarzschild-mirror system, which has not been studied even with the scalar-like boundary conditions. To this end, we first formulate the Maxwell equations on the Schwarzschild background by using the Regge-Wheeler-Zerilli approach [35, 36] and then, based on the vanishing energy flux principle, derive *two* sets of explicit boundary conditions at the mirror's location and accordingly obtain *two* branches of quasinormal spectrum. For the pure cavity case, QNMs turn into normal modes and which are solved analytically. For the case of BHs in a cavity, the Maxwell QNMs are solved numerically by using two different approaches and we present the results by varying the mirror radius r_m , the angular momentum quantum number ℓ and the overtone number N . In particular, we disclose that the Maxwell spectrum may *bifurcate* on the Schwarzschild BHs in a mirror-like cavity under the vanishing energy flux boundary conditions.

^{*} Corresponding author: mjwang@hunnu.edu.cn.

This paper is organized as follows. In Section II we present the Maxwell equations on the Schwarzschild background in the Regge-Wheeler-Zerilli formalism, and derive the corresponding boundary conditions for a BH-mirror system, following the vanishing energy flux principle. In Section III we first introduce a pseudospectral method and a matrix method, and then apply them to explore the Maxwell quasinormal spectrum numerically and, in particular, demonstrate that the vanishing energy flux principle leads to *two* sets of modes and for both modes they may *bifurcate* when varying the mirror radius. Final remarks and conclusions are devoted in Section V, and we leave an analytic calculation on the normal modes of the Maxwell fields in a pure cavity in the Appendix.

II. MAXWELL EQUATIONS AND BOUNDARY CONDITIONS

In this section, we briefly review equations of motion for the Maxwell fields on Schwarzschild BHs in the Regge-Wheeler-Zerilli formalism and, based on the vanishing energy flux principle, derive the corresponding boundary conditions at the location of a mirror.

A. The Maxwell equations

We start by considering the Schwarzschild geometry with the following line element

$$ds^2 = f(r)dt^2 - \frac{1}{f(r)}dr^2 - r^2(d\theta^2 + \sin^2\theta d\varphi^2), \quad (1)$$

with the metric function

$$f(r) \equiv 1 - \frac{2M}{r}, \quad (2)$$

where M is the ADM mass, and the event horizon, determined by $f(r_+) = 0$, is $r_+ = 2M$.

The Maxwell equations are given by

$$\nabla_\nu F^{\mu\nu} = 0, \quad (3)$$

where the field strength tensor is defined as $F_{\mu\nu} = \partial_\mu A_\nu - \partial_\nu A_\mu$. In the Regge-Wheeler-Zerilli formalism [35, 36], the vector potential A_μ may be decomposed in terms of the scalar and vector spherical harmonics [37]

$$A_\mu = e^{-i\omega t} \sum_{\ell, m} \left(\begin{bmatrix} 0 \\ 0 \\ a^{\ell m}(r) \mathbf{S}_{\ell m} \end{bmatrix} + \begin{bmatrix} j^{\ell m}(r) Y_{\ell m} \\ h^{\ell m}(r) Y_{\ell m} \\ k^{\ell m}(r) \mathbf{Y}_{\ell m} \end{bmatrix} \right), \quad (4)$$

where $Y_{\ell m}$ are the scalar spherical harmonics, $\mathbf{S}_{\ell m}$ and $\mathbf{Y}_{\ell m}$ are the vector spherical harmonics with the definitions

$$\mathbf{S}_{\ell m} = \begin{pmatrix} \frac{1}{\sin\theta} \partial_\varphi Y_{\ell m} \\ -\sin\theta \partial_\theta Y_{\ell m} \end{pmatrix}, \quad \mathbf{Y}_{\ell m} = \begin{pmatrix} \partial_\theta Y_{\ell m} \\ \partial_\varphi Y_{\ell m} \end{pmatrix},$$

and where ω is the frequency, ℓ is the angular momentum quantum number, m is the azimuthal number. Considering the symmetry of the spherical harmonics under the transformations $(\theta, \varphi) \rightarrow (\pi - \theta, \pi + \varphi)$, the first (second) column in the right hand side of Eq. (4) has parity $(-1)^{\ell+1}$ ($(-1)^\ell$), so that we shall call the former (latter) the axial (polar) modes.

By substituting Eq. (4) into Eq. (3), one obtains the radial part of the Maxwell equations which, by using the tortoise coordinate

$$\frac{dr_*}{dr} = \frac{1}{f(r)}, \quad (5)$$

may be written in the Schrödinger-like form

$$\left(\frac{d^2}{dr_*^2} + \omega^2 - \ell(\ell+1) \frac{f(r)}{r^2} \right) \Psi(r) = 0, \quad (6)$$

where for axial modes

$$\Psi(r) = a^{\ell m}(r),$$

and for polar modes

$$\Psi(r) = \frac{r^2}{\ell(\ell+1)} \left(-i\omega h^{\ell m}(r) - \frac{dj^{\ell m}(r)}{dr} \right).$$

B. Boundary conditions

The Maxwell QNMs are determined by Eq. (6) with physically motivated boundary conditions. In this paper, we consider a BH-mirror system, so that one has to impose boundary conditions both at the horizon and at a mirror's location. At the horizon, we impose an ingoing wave boundary condition as usual. By placing a mirror at a finite radius r_m and considering a perfectly reflecting mirror, we require that the energy flux of the Maxwell fields should be vanished at r_m , following a generic principle we proposed for asymptotically AdS black holes in [28] (see also [32, 38]).

To this end, by starting from the energy-momentum tensor of the Maxwell field

$$T_{\mu\nu} = F_{\mu\sigma} F^\sigma{}_\nu + \frac{1}{4} g_{\mu\nu} F^2, \quad (7)$$

one may obtain the spatial part of the radial energy flux, which is given by

$$\mathcal{F}|_r \propto f(r) \Psi(r) \Psi'(r), \quad (8)$$

where \prime denotes a derivative with respect to r . Then the vanishing energy flux principle employed at a finite radius, i.e. $\mathcal{F}|_{r_m} = 0$, leads to the following two solutions

$$\Psi(r)|_{r=r_m} = 0, \quad (9)$$

$$\Psi'(r)|_{r=r_m} = 0, \quad (10)$$

where r_m is again the mirror radius in the Schwarzschild coordinates. The above two conditions indicate *two* sets

of quasinormal spectrum and, as we will show in the numeric calculations, that they are dissimilar as well. Moreover, the conditions given by Eqs. (9) and (10) are exactly the same with those obtained by treating the mirror as a conductor [39].

III. METHODS

In order to study the Maxwell QNMs in a full parameter space, one has to resort to numeric methods. In this section, we briefly introduce two numeric methods used in this paper to generate data, i.e. a pseudospectral method [40] and a matrix method [41, 42].

A. Pseudospectral method

This method has been successfully employed to look for the Maxwell quasinormal spectrum on asymptotically AdS spacetimes [30], and here we follow closely the prescription given in [30] but adapted with boundary conditions for the mirror case.

We first, for numeric convenience, make the transformation

$$\Psi = e^{-i\omega r_*} \phi, \quad (11)$$

where the tortoise coordinate r_* is defined in Eq. (5), which brings Eq. (6) from a quadratic eigenvalue problem into a linear eigenvalue problem.

Furthermore, by changing the coordinate from r to z through

$$z = 1 - 2 \frac{r_m - r}{r_m - r_+}, \quad (12)$$

the integration domain is then transformed from $r \in [r_+, r_m]$ to $z \in [-1, +1]$, and Eq. (6) turns into the form

$$\mathcal{B}_0(z)\phi(z) + \mathcal{B}_1(z, \omega)\phi'(z) + \mathcal{B}_2(z)\phi''(z) = 0, \quad (13)$$

where the functions $\mathcal{B}_j (j = 0, 1, 2)$ may be derived straightforwardly by substituting Eqs. (11) and (12) into Eq. (6), and where \prime denotes a derivative with respect to z . One should note that here \mathcal{B}_1 is a linear function of ω , i.e. $\mathcal{B}_1(z, \omega) = \mathcal{B}_{1,0}(z) + \omega \mathcal{B}_{1,1}(z)$.

Then one may discretize Eq. (13) by introducing the Chebyshev points

$$z_j = \cos\left(\frac{j\pi}{n}\right), \quad j = 0, 1, \dots, n, \quad (14)$$

where n denotes the number of grid points, and obtain an algebraic equation

$$(M_0 + \omega M_1)\phi(z) = 0, \quad (15)$$

where the matrices M_0 and M_1 are composed of the functions $\mathcal{B}_j (j = 0, 1, 2)$ and the Chebyshev differential matrices [40].

To solve the eigenvalue equation (15), one has to impose physically relevant boundary conditions both at the horizon and at a mirror's location. At the horizon, we impose a regular boundary condition for ϕ , since an ingoing wave boundary condition for Ψ is guaranteed by Eq. (11). At a mirror's position, from Eq. (11), boundary conditions given by Eqs. (9) and (10) are transformed into

$$\phi(1) = 0, \quad (16)$$

$$\phi'(1) - \frac{i\omega r_m}{2}\phi(1) = 0, \quad (17)$$

where

$$\phi'(1) \equiv \frac{d\phi(z)}{dz}\bigg|_{z=1}.$$

B. Matrix method

The Maxwell quasinormal spectrum may be also calculated by using a matrix method [41, 42], and here we briefly describe this method.

Similarly to the pseudospectral method introduced in the above, we first make the transformation given by Eq. (11) so that an ingoing wave boundary condition at the horizon is satisfied for Ψ automatically.

Then we make a coordinate transformation

$$x = \frac{r - r_+}{r_m - r_+}, \quad (18)$$

which brings the integration domain from $r \in [r_+, r_m]$ to $x \in [0, 1]$. We further implement the transformation from ϕ to χ through

$$\chi(x) = x\phi(x), \quad (19)$$

such that the boundary condition at the event horizon becomes

$$\chi(0) = 0, \quad (20)$$

and then Eq. (6) becomes

$$\tilde{\mathcal{B}}_0(x, \omega)\chi(x) + \tilde{\mathcal{B}}_1(x, \omega)\chi'(x) + \tilde{\mathcal{B}}_2(x)\chi''(x) = 0, \quad (21)$$

where the functions $\tilde{\mathcal{B}}_j (j = 0, 1, 2)$ may be derived directly by substituting Eqs. (11), (18) and (19) into Eq. (6). Note that here $\tilde{\mathcal{B}}_j (j = 0, 1)$ are linear functions of ω , i.e. $\tilde{\mathcal{B}}_j(x, \omega) = \tilde{\mathcal{B}}_{j,0}(x) + \omega \tilde{\mathcal{B}}_{j,1}(x)$.

To discretize Eq. (21) by using the matrix method, it is used to introduce equally spaced grid points in the interval $[0, 1]$. The corresponding differential matrices may be constructed by using the Taylor series to expand the function $\chi(x)$ around each grid point. Then Eq. (21) becomes an algebraic equation in the matrix form

$$(\tilde{M}_0 + \omega \tilde{M}_1)\chi(x) = 0, \quad (22)$$

where \tilde{M}_0 and \tilde{M}_1 are matrices composed by the functions $\tilde{B}_j(j = 0, 1, 2)$ and the corresponding differential matrices, and the explicit form of these matrices may be found in [41, 42].

To solve the eigenfrequencies from Eq. (22), apart from the boundary condition at the horizon given in Eq. (20), one has to impose boundary conditions at a mirror's location. Considering the transformations we made in Eqs. (11) and (19), boundary conditions given by Eqs. (9) and (10) are then transformed into

$$\chi(1) = 0, \quad (23)$$

$$\chi'(1) - (1 + i\omega r_m) \chi(1) = 0, \quad (24)$$

where

$$\chi'(1) \equiv \left. \frac{d\chi(x)}{dx} \right|_{x=1}.$$

IV. RESULTS

With the numeric methods illustrated above at hand, one may obtain the Maxwell quasinormal spectrum on Schwarzschild BHs in a cavity. In the numeric calculations we take the event horizon $r_+ = 1$ to measure all other physical quantities. Moreover, we use ω_1 (ω_2) to represent QNMs corresponding to the first (second) boundary condition given by Eq. (9) (Eq. (10)), and introduce ℓ and N to denote the angular momentum quantum number and the overtone number.

We first display both real and imaginary parts of the Maxwell QNMs in terms of the mirror radius r_m with both boundary conditions in Fig. 1, by taking $\ell = 1$ and $N = 0, 1, 2$ as examples. From this figure, we confirm that the vanishing energy flux principle is applicable to a BH-mirror system and leads to *two* different branches of modes. It shows clearly that, for both boundary conditions with fixed ℓ and N , the magnitude of real (imaginary) part of QNMs first increases up to a maximum and then decreases (always increases), as the mirror approaches the event horizon. By increasing the mirror radius r_m , the magnitude of real part of QNMs for both boundary conditions asymptotes to the corresponding normal modes in a pure cavity, given by Eqs. (A4) and (A5) as calculated in Appendix. A, while the imaginary part may be computed perturbatively by using a standard analytic matching method [43]. Here we compare analytic results with numeric data in Table I, but leave detailed calculations for the analytic results elsewhere. We find a good agreement between analytic and numeric results for large r_m , which not only verifies the validity of the analytic calculations but also checks our numeric data.

By zooming Fig. 1 around the event horizon, one observes an absorbing feature in Fig. 2 that the Maxwell spectrum may *bifurcate*. To be precise, as shown in Fig. 2, we find out that for both boundary conditions when the real part of QNMs becomes *zero*, which de-

TABLE I. A comparison for the imaginary part of the Maxwell QNMs between analytic results with the first ($-\Im\omega_{1a}$) and second ($-\Im\omega_{2a}$) boundary conditions and numeric data with the first ($-\Im\omega_{1n}$) and second ($-\Im\omega_{2n}$) boundary conditions. Here we take $N = 0$ and $\ell = 1$ but vary r_m . Notice that the larger mirror radius the better agreement between analytic and numeric results. Also note that, with fixed r_m , the agreement with the second boundary is better than the agreement with the first boundary.

r_m	$-\Im\omega_{1n}$	$-\Im\omega_{1a}$	$-\Im\omega_{2n}$	$-\Im\omega_{2a}$
80	1.598×10^{-8}	1.469×10^{-8}	2.399×10^{-9}	2.326×10^{-9}
160	4.726×10^{-10}	4.548×10^{-10}	7.345×10^{-11}	7.244×10^{-11}
220	9.492×10^{-11}	9.240×10^{-11}	1.487×10^{-11}	1.473×10^{-11}

termines a critical mirror radius r_m^c ,¹ the imaginary part *branches off* into two sets of modes when r_m is smaller than r_m^c . This phenomenon, we dubbed as the *mode split* effect, has also been reported for the Maxwell fields on asymptotically AdS BHs [30]. By using the same terminology introduced in [30], we term, in magnitude, the larger (smaller) one of the two sets of modes as the upper (lower) mode. The upper (lower) mode, for both boundary conditions, increases (decreases) as r_m approaches the event horizon, and it varies weakly with r_m when the mirror radius is smaller than and away from the critical mirror radius. In particular, when the mirror radius r_m is close to the event horizon, one may achieve a very simple structure of the modes, that is the upper (lower) mode with the first boundary condition asymptotes to $-(N+1)i$ [$-(N+0.5)i$], while with the second boundary the upper (lower) mode asymptotes to $-(N+0.5)i$ [$-Ni$].

The impact of the overtone number N on the spectrum varies with the mirror position. When the mirror radius is greater than and away from the critical mirror radius, as shown in Fig. 1, with a fixed r_m for both boundary conditions, the magnitude for both real and imaginary parts of QNMs increase as N increases; while when the mirror is placed around the critical mirror radius, as shown in Fig. 2, with a fixed r_m for both boundary conditions, the magnitude for real part of QNMs decreases but the imaginary part increases (for both upper and lower modes) as N increases. Moreover, as shown in Fig. 2, the critical mirror radius for both boundary conditions increases as N increases.

We also explore the Maxwell spectrum in terms of r_m for both boundary conditions with fixed N but various ℓ in Fig. 3, by taking $N = 0$ and $\ell = 1, 2, 3$ as examples. The general behavior is quite similar to Fig. 1. Again

¹ Note that, by fixing all other parameters, the critical mirror radius with the first boundary r_{m1}^c is greater than the counterpart with the second boundary r_{m2}^c .

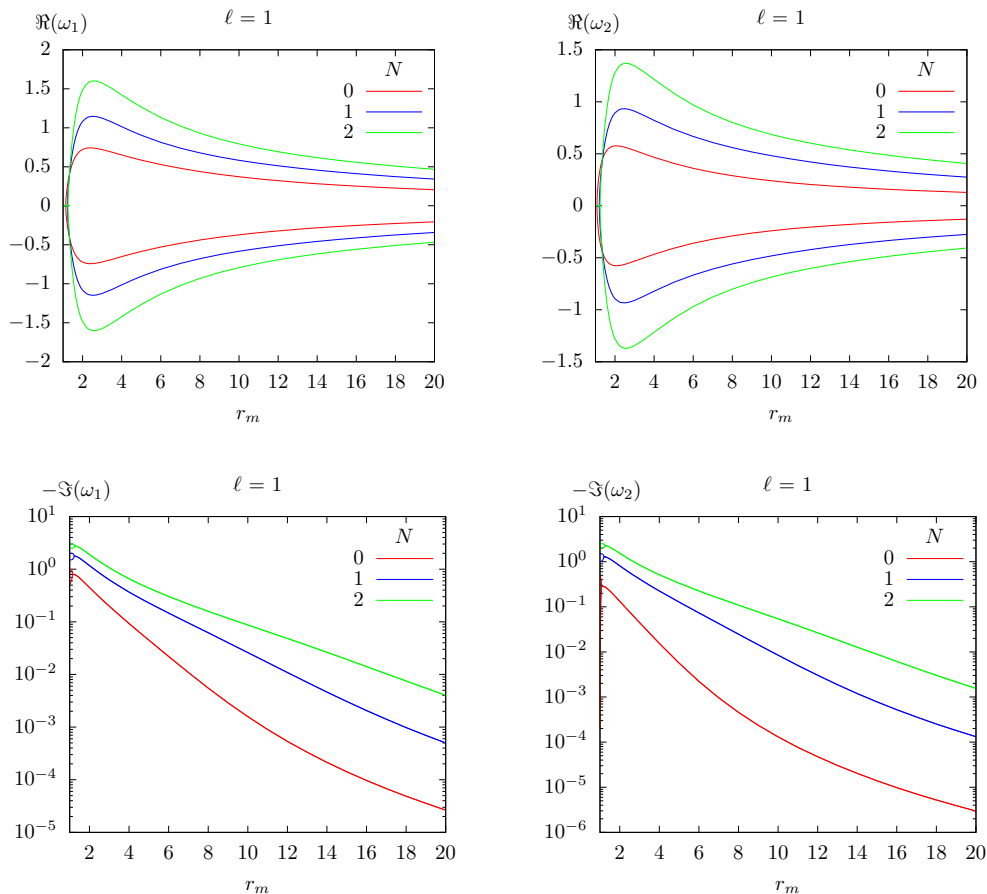


FIG. 1. Real (top) and imaginary (bottom) parts of the Maxwell QNMs on Schwarzschild BHs in a cavity vs the mirror radius r_m , for $\ell = 1$ and $N = 0$ (red), 1 (blue), 2 (green), with the first (left) and second (right) boundary conditions. Note that in the bottom panels for imaginary part of QNMs with both boundary conditions, we use the semilogarithmic coordinates.

by zooming Fig. 3 around the event horizon, we have Fig. 4 which shows that the mode split effect does *exist* not only for various values of N but also for different values of ℓ . By increasing ℓ , shown in Figs. 3 and 4 for both boundary conditions, the magnitude of real part of QNMs always increases; while the magnitude of imaginary part decreases (increases) when r_m is away from (around) r_m^c . Moreover, as shown in Fig. 4 and contrary to N effects, the critical mirror radius for both boundary conditions decreases as ℓ increases, and by fixing all other parameters the critical mirror radius with the first boundary condition is again greater than the counterpart with the second boundary condition. In particular, the modes for different ℓ with both boundary conditions are *degenerate*, as the mirror approaches the event horizon, which is again contradictory to N effects.

V. DISCUSSION AND FINAL REMARKS

In this paper, we have studied the Maxwell quasinormal spectrum on Schwarzschild BHs in a mirror-like cav-

ity, by imposing the vanishing energy flux boundary conditions. We have shown that the vanishing energy flux principle is applicable to a BH-mirror system and leads to two distinct branches of modes. In particular, we demonstrated that the spectrum may *bifurcate*, which shows, as an example among others, the similarity between BH-mirror and BH-AdS systems. More specifically, we unveiled that for both boundary conditions, when the mirror radius r_m is less than the corresponding critical mirror radius r_m^c , the real part of the Maxwell QNMs *vanishes* while the imaginary part *branches off*. This feature is prominent when the mirror is placed close to the event horizon. We also found that, with fixed other parameters, the critical mirror radius with the first boundary condition is greater than the counterpart with the second boundary condition.

When the mirror radius is greater than and away from the corresponding critical mirror radius, we observed the following trends of the Maxwell spectrum. With fixed ℓ and N , the magnitude of real (imaginary) part of QNMs for both boundary conditions first increases and then decreases (increases) as the mirror radius r_m approaches

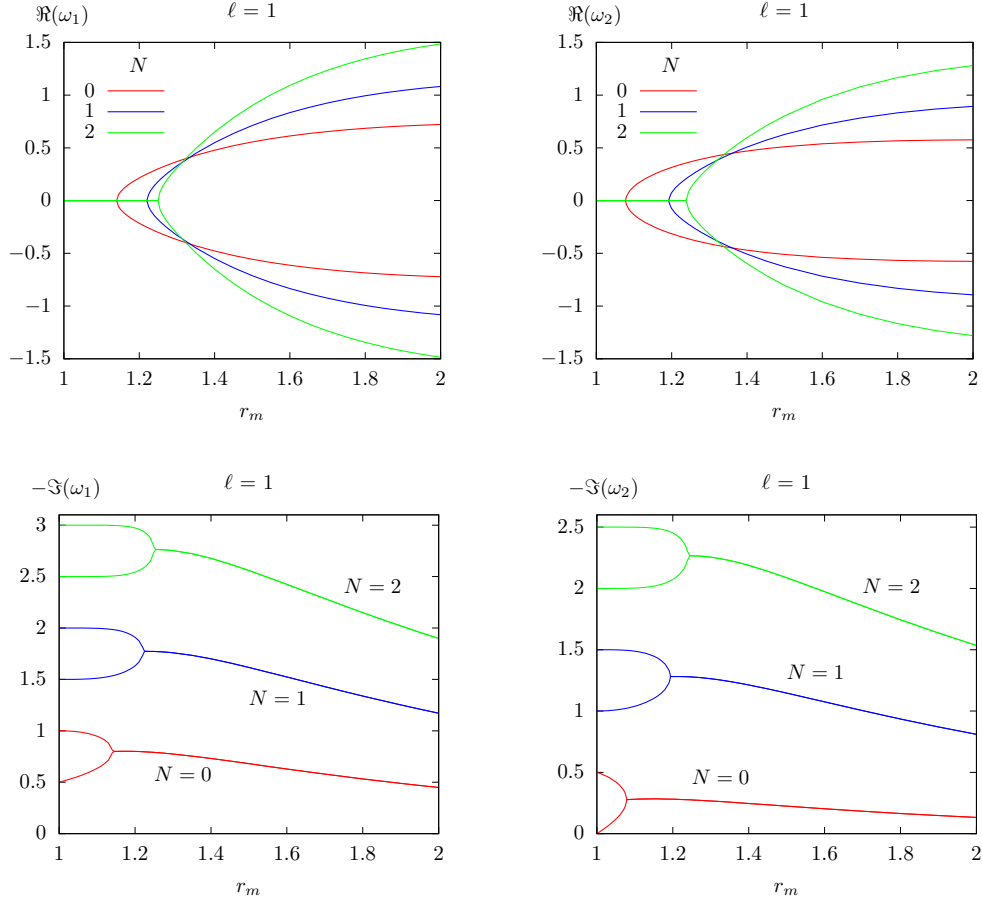


FIG. 2. This figure is obtained by zooming Fig. 1 around the event horizon to better display the spectrum bifurcation of the Maxwell fields on Schwarzschild BHs in a cavity for both boundary conditions.

the event horizon r_+ . With fixed r_m and ℓ , the magnitude of real (imaginary) part of QNMs for both boundary conditions increases (increases) as N increases; while with fixed r_m and N , the magnitude of real (imaginary) part of QNMs for both boundary conditions increases (decreases) as ℓ increases. When the mirror radius is around the critical mirror radius, on the other hand, the impact of N on the real (imaginary) part of the spectrum is opposite (same) to the former case while the impact of ℓ on the real (imaginary) part of the spectrum is same (opposite) to the former case. Moreover, we observed that the critical mirror radius, for both boundary conditions, increases as N increases but decreases as ℓ increases.

By adding rotation to the background, superradiance and the corresponding instabilities may be triggered. It is then particularly interesting to investigate the interaction between superradiant instabilities and the spectrum bifurcation. Work along these directions is underway and we hope to report on them soon.

Acknowledgements. This work is supported by the National Natural Science Foundation of China under Grant Nos. 11705054, 11881240252, 12035005, and by the Hu-

nan Provincial Natural Science Foundation of China under Grant Nos. 2018JJ3326.

Appendix A: The Maxwell normal modes in a cavity

In this appendix, we look for the Maxwell normal modes by solving Eq. (6) in a cavity *analytically*, with vanishing energy flux boundary conditions given by Eqs. (9) and (10).

For the cavity case, the Maxwell equation (6) becomes

$$\left(\frac{d^2}{dr^2} + \omega^2 - \frac{\ell(\ell+1)}{r^2} \right) \Psi(r) = 0, \quad (\text{A1})$$

which leads to the solution

$$\Psi(r) \sim \sqrt{r} \left(c_1 J_{\ell+\frac{1}{2}}(\omega r) + c_2 Y_{\ell+\frac{1}{2}}(\omega r) \right), \quad (\text{A2})$$

where $J_\nu(z)$ and $Y_\nu(z)$ are the first kind and second kind Bessel functions, respectively.

By expanding the solution (A2) at the origin and by imposing regularity condition, we shall set $c_2 = 0$ and

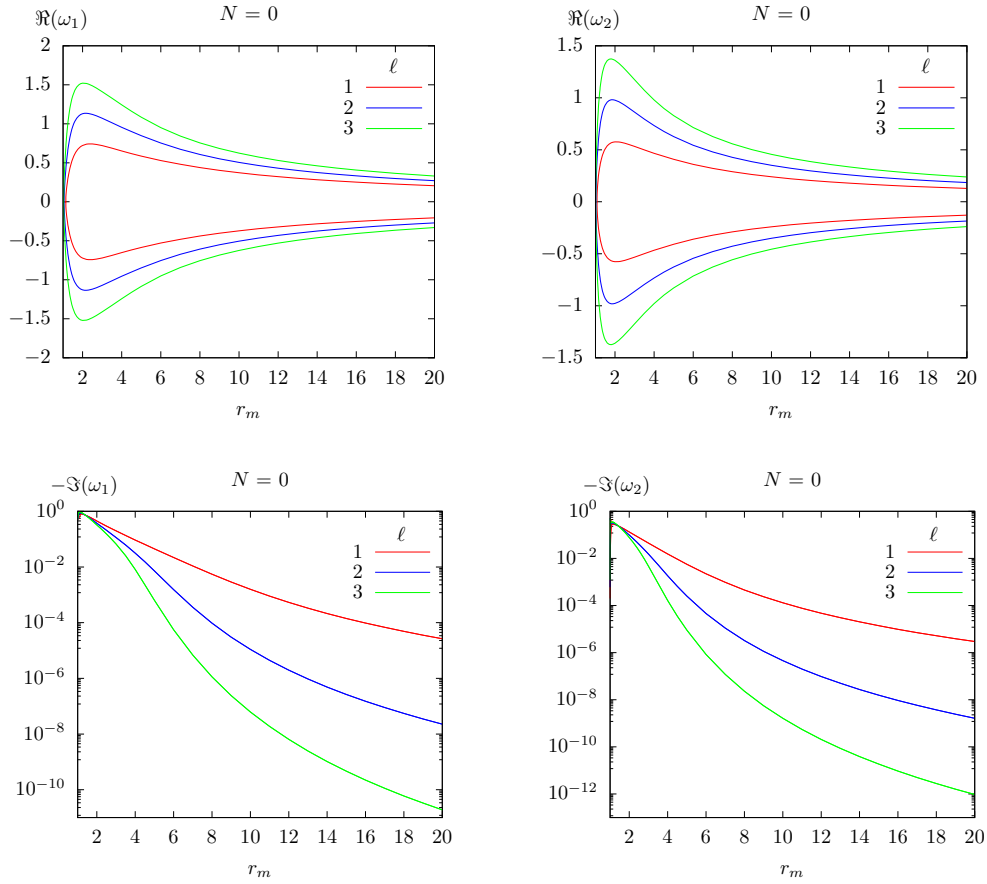


FIG. 3. Real (top) and imaginary (bottom) parts of the Maxwell QNMs on Schwarzschild BHs in a cavity vs the mirror radius r_m , for $N = 0$ and $\ell = 1$ (red), 2 (blue), 3 (green), with the first (left) and second (right) boundary conditions. Note that in the bottom panels for imaginary part of QNMs with both boundary conditions, we use the semilogarithmic coordinates.

get

$$\Psi(r) \sim \sqrt{r} J_{\ell+\frac{1}{2}}(\omega r). \quad (\text{A3})$$

Then the boundary condition (9) leads to

$$\omega_1 r_m = j_{\ell+\frac{1}{2},N}, \quad (\text{A4})$$

while the boundary condition (10) leads to

$$\omega_2 r_m = \tilde{j}_{\ell+\frac{1}{2},N}. \quad (\text{A5})$$

Here $j_{\nu,N}$ and $\tilde{j}_{\nu,N}$ denote zeros of the Bessel function $J_\nu(\omega r)$ and zeros of $\partial_r[\sqrt{r}J_\nu(\omega r)]|_{r_m}$, and N is the overtone number.

As one may observe that two normal modes, obtained in Eqs (A4) and (A5), are *different*, which is contradictory to the AdS case where two normal modes are the same up to one mode [28]. Moreover, these two normal modes obtained by imposing the vanishing energy flux boundary conditions are exactly the same with those obtained by imposing the conductor condition [39].

-
- [1] LIGO Scientific, Virgo, B. P. Abbott *et al.*, Phys. Rev. Lett. **116**, 061102 (2016), [1602.03837].
 - [2] LIGO Scientific, Virgo, B. P. Abbott *et al.*, Phys. Rev. Lett. **116**, 241102 (2016), [1602.03840].
 - [3] LIGO Scientific, Virgo, B. P. Abbott *et al.*, Phys. Rev. Lett. **116**, 221101 (2016), [1602.03841], [Erratum: Phys.Rev.Lett. 121, 129902 (2018)].
 - [4] LIGO Scientific, Virgo, B. P. Abbott *et al.*, Phys. Rev. Lett. **116**, 241103 (2016), [1606.04855].

- [5] LIGO Scientific, Virgo, B. P. Abbott *et al.*, Phys. Rev. Lett. **119**, 141101 (2017), [1709.09660].
- [6] LIGO Scientific, Virgo, R. Abbott *et al.*, Phys. Rev. Lett. **125**, 101102 (2020), [2009.01075].
- [7] Event Horizon Telescope, K. Akiyama *et al.*, Astrophys. J. Lett. **875**, L1 (2019), [1906.11238].
- [8] Event Horizon Telescope, K. Akiyama *et al.*, Astrophys. J. Lett. **875**, L4 (2019), [1906.11241].
- [9] Event Horizon Telescope, K. Akiyama *et al.*, Astrophys.

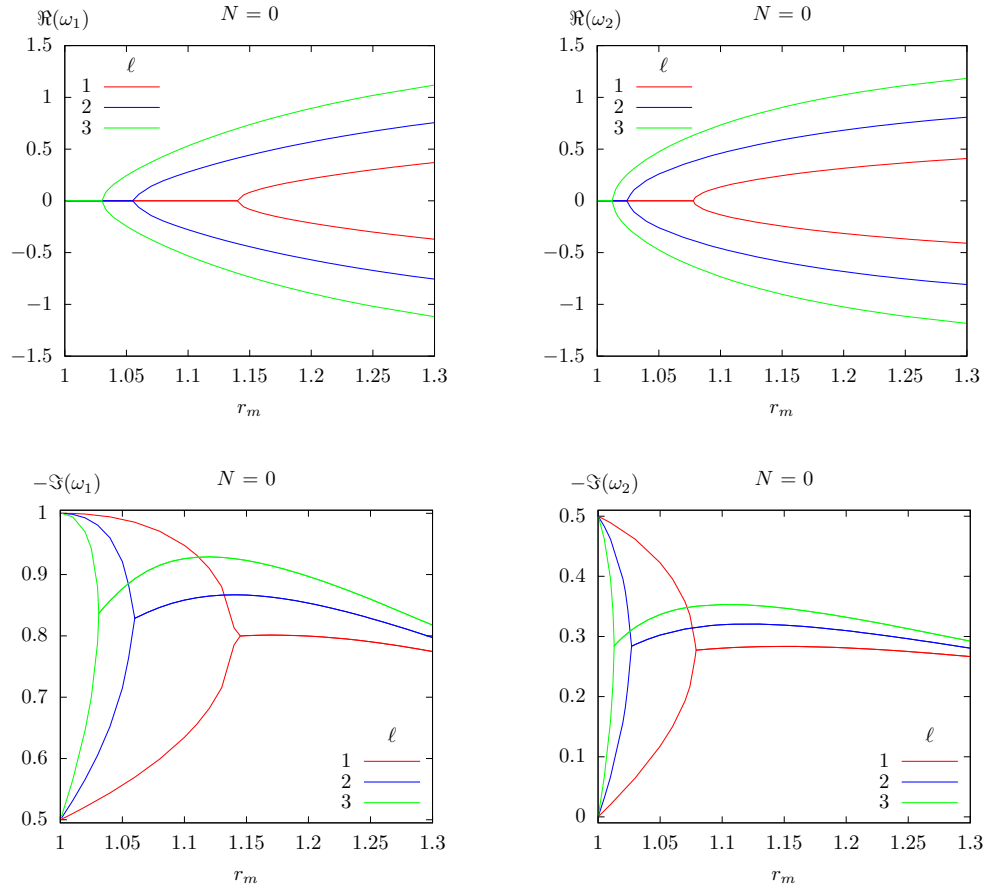


FIG. 4. Spectrum bifurcation of the Maxwell fields on Schwarzschild BHs in a cavity for both boundary conditions with fixed N but with different ℓ . Note that this figure is obtained by zooming Fig. 3 around the event horizon.

- J. Lett. **875**, L5 (2019), [1906.11242].
- [10] Event Horizon Telescope, K. Akiyama *et al.*, *Astrophys. J. Lett.* **875**, L6 (2019), [1906.11243].
- [11] V. Ferrari and L. Gualtieri, *Gen. Rel. Grav.* **40**, 945 (2008), [0709.0657].
- [12] E. Berti, K. Yagi, H. Yang and N. Yunes, *Gen. Rel. Grav.* **50**, 49 (2018), [1801.03587].
- [13] K. Jusufi, *Phys. Rev. D* **101**, 084055 (2020), [1912.13320].
- [14] H. Yang, *Phys. Rev. D* **103**, 084010 (2021), [2101.11129].
- [15] K. D. Kokkotas and B. G. Schmidt, *Living Rev. Rel.* **2**, 2 (1999), [gr-qc/9909058].
- [16] H.-P. Nollert, *Class. Quant. Grav.* **16**, R159 (1999).
- [17] E. Berti, V. Cardoso and A. O. Starinets, *Class. Quant. Grav.* **26**, 163001 (2009), [0905.2975].
- [18] R. Konoplya and A. Zhidenko, *Rev. Mod. Phys.* **83**, 793 (2011), [1102.4014].
- [19] G. T. Horowitz and V. E. Hubeny, *Phys. Rev. D* **62**, 024027 (2000), [hep-th/9909056].
- [20] J. Chan and R. B. Mann, *Phys. Rev. D* **55**, 7546 (1997), [gr-qc/9612026].
- [21] J. Chan and R. B. Mann, *Phys. Rev. D* **59**, 064025 (1999).
- [22] V. Cardoso and J. P. Lemos, *Phys. Rev. D* **64**, 084017 (2001), [gr-qc/0105103].
- [23] V. Cardoso, R. Konoplya and J. P. Lemos, *Phys. Rev. D* **68**, 044024 (2003), [gr-qc/0305037].
- [24] E. Berti and K. Kokkotas, *Phys. Rev. D* **67**, 064020 (2003), [gr-qc/0301052].
- [25] M. Giammatteo and J.-l. Jing, *Phys. Rev. D* **71**, 024007 (2005), [gr-qc/0403030].
- [26] J.-l. Jing, *gr-qc/0502010*.
- [27] J.-l. Jing and Q.-y. Pan, *Phys. Rev. D* **71**, 124011 (2005), [gr-qc/0502011].
- [28] M. Wang, C. Herdeiro and M. O. P. Sampaio, *Phys. Rev. D* **92**, 124006 (2015), [1510.04713].
- [29] M. Wang and C. Herdeiro, *Phys. Rev. D* **93**, 064066 (2016), [1512.02262].
- [30] M. Wang, Z. Chen, X. Tong, Q. Pan and J. Jing, *Phys. Rev. D* **103**, 064079 (2021), [2104.04970].
- [31] M. Wang, Z. Chen, Q. Pan and J. Jing, *Eur. Phys. J. C* **81**, 469 (2021), [2105.10951].
- [32] M. Wang, *Int. J. Mod. Phys. D* **25**, 1641011 (2016).
- [33] M. Wang, C. Herdeiro and J. Jing, *Phys. Rev. D* **96**, 104035 (2017), [1710.10461].
- [34] M. Wang, C. Herdeiro and J. Jing, *Phys. Rev. D* **100**, 124062 (2019), [1910.14305].
- [35] T. Regge and J. A. Wheeler, *Phys. Rev.* **108**, 1063 (1957).
- [36] F. J. Zerilli, *Phys. Rev. Lett.* **24**, 737 (1970).
- [37] R. Ruffini, *Black Holes: les Astres Occlus*. Gordon and Breach Science Publishers, New York, 1973.
- [38] M. Wang, *Quantum and classical aspects of scalar and*

- vector fields around black holes*, PhD thesis, Aveiro U., 2016, 1606.00811.
- [39] R. Brito, V. Cardoso and P. Pani, Lect. Notes Phys. **906**, pp.1 (2015), [1501.06570].
- [40] L. N. Trefethen, *Spectral methods in MATLAB* (Siam, 2000).
- [41] K. Lin and W.-L. Qian, Class. Quant. Grav. **34**, 095004 (2017), [1610.08135].
- [42] K. Lin, W.-L. Qian, A. B. Pavan and E. Abdalla, Mod. Phys. Lett. A **32**, 1750134 (2017), [1703.06439].
- [43] M. Wang and C. Herdeiro, Phys.Rev. **D89**, 084062 (2014), [1403.5160].